ISSN 2176-5480

22nd International Congress of Mechanical Engineering (COBEM 2013)
November 3-7, 2013, Ribeirão Preto, SP, Brazil

DIFFRACTION EFFECTS OF FINITE AND SEMI-INFINITE FLAT PLATES IN THE VICINITY OF A TURBULENT SUBSONIC JET

André V. G. Cavalieri
Institut Pprime, 43 rue de l'Aérodrome, 86036 Poitiers, France
Instituto Tecnológico de Aeronáutica, Divisão de Engenharia Aeronáutica, Praça Mal. Eduardo Gomes, 50, 12228-900, São José dos Campos - SP, Brazil
andre@ita.br
William R. Wolf
Universidade Estadual de Campinas, Faculdade de Engenharia Mecânica, Departamento de Energia, Rua Mendeleyev, 200, 13083-970, Campinas - SP, Brazil
wolf@fem.unicamp.br
Peter Jordan **Yves Gervais**
Institut Pprime, 43 rue de l'Aérodrome, 86036 Poitiers, France
peter.jordan@univ-poitiers.fr yves.gervais@univ-poitiers.fr

Abstract. *We present an investigation of the acoustic scattering due to the presence of a flat plate in the vicinity of a turbulent subsonic jet. Experiments have been performed to measure sound fields for Mach numbers ranging from 0.4 to 0.6, and for distances between the plate and the jet axis ranging from 1 to 2 jet diameters. The acoustic results include a significant increase in the low-frequency sound radiation, and phase opposition between the shielded and unshielded sides of the plate. There is an exponential decay of the scattered sound with increasing jet-plate distance, suggesting that low-frequency radiation is due to the scattering of evanescent hydrodynamic wavepackets in the jet near field. To model this phenomenon, we calculate sound generation from wave-packet sources in two ways: on one hand we use a tailored Green's function that accounts for the presence of a semi-infinite, rigid flat plate; and, on the other, we solve numerically the Helmholtz equation, with boundary conditions representative of a finite flat plate, using a fast multipole boundary element method. In agreement with the experimental measurements, numerical calculations capture the phase opposition between shielded and unshielded sides, and the scattered sound depends exponentially on the position of the plate. This exponential dependence is related to non-compact effects associated with wavepackets, as compact sources would lead to an algebraic dependence. Acoustic pressure directivities computed for the finite and semi-infinite flat plates agree well where acoustic reflection and diffraction from the trailing edge of the plates are concerned. However, additional diffraction effects associated with the leading and lateral edges of the finite plate, and which take the form of multiple lobes in the directivity, are illustrated by the comparison. As the plate dimensions are increased, i.e. the Helmholtz number is increased, the solution approaches that obtained for the semi-infinite plate.*

Keywords: *aeroacoustics, jet noise, acoustic scattering, trailing edge noise*

1. INTRODUCTION

The calculation of noise radiated by jets exiting aircraft engines in the vicinity of a wing is a problem involving both sound generation by turbulence in the jet and scattering by the surfaces: it is important to understand how the neighbouring surfaces modify the sound radiation in order to evaluate how the installation of the engine on an aircraft will impact the radiated noise. Among the first attempts to study surface effects in aeroacoustics was the work of Curle (1955), who extended Lighthill's acoustic analogy (Lighthill, 1952) to account for acoustic scattering effects due to the presence of solid surfaces.

The use of a free-field Green's function to obtain the solution of Curle's equation leads to integrals involving the pressure and its normal derivative evaluated on the solid surfaces, as well as the usual volume integral that appears in the free-jet case. If the pressure on the wing surface, assumed as rigid, is known, Curle's approach can be used to determine the radiated sound. However, if jet and wing are sufficiently close, the fluctuating pressure on the wing surface will depend on jet turbulence. An alternative to Curle's method is to use a Green's function tailored to the geometry of the problem. In this approach, the calculation of the radiated sound can be performed without the surface pressure distribution. This approach was considered by Ffowcs Williams and Hall (1970), who studied sound radiation in the presence of a semi-infinite flat plate. The tailored Green's function for this geometry is available (Macdonald, 1915), and allows a study of the effects of the plate on sound generation by turbulence modelled as compact eddies. The noise radiated by compact quadrupoles close to the plate edge is seen to be significantly enhanced due to scattering by the surface. For the installed

ISSN 2176-5480

jet problem, this issue is of relevance, for the wing trailing edge should behave in a similar manner.

The applicability of Ffowcs Williams & Hall's results to the installed jet problem may be questioned due to the assumption of compact sources. Indeed, a number of researchers have postulated that instability waves, or wavepackets, are related to sound radiation at shallow angles; for instance, see Crow (2072), Ffowcs Williams and Kempton (1978) or Mankbadi and Liu (1984) to name just a few. Recent work has confirmed that the acoustic field of subsonic jets has the superdirectivity expected in wavepacket radiation (Cavalieri *et al.*, 2012a). Moreover, experiments have demonstrated that natural free jets comprise hydrodynamic wavepackets extending several jet diameters (Suzuki and Colonius, 2006; Gudmundsson and Colonius, 2011; Cavalieri *et al.*, 2012b). A review of the role of wave-packets in turbulent jet noise is provided by Jordan and Colonius (2013).

In this work, an investigation of the installation effects presented by the proximity of an aircraft wing to its propulsive jet is undertaken by means of experimental measurement, analysis and modelling. A simplified experimental configuration is considered, comprising a single-stream isothermal jet in static conditions, the wing being mimicked by a flat plate that acts as a diffractive surface. The configuration is similar to that of Mead and Strange (1998) and Lawrence *et al.* (2011). The effect of jet-wing distance on the radiated sound is assessed as a function of Mach number. The acoustic signature of the system is analysed by means of two farfield microphones, disposed (see figure 1) so as to allow the signature of the scattered field, with a phase opposition between shielded and unshielded sides, to be easily identified.

The aeroacoustic problem is subsequently modelled using wave-packet sources educed in previous experiments using the same jets in free-field conditions. The sound field is computed in two ways, using a tailored Green's function that accounts for the presence of a semi-infinite, rigid flat plate (Macdonald, 1915; Ffowcs Williams and Hall, 1970), and by solution of the Helmholtz equation with boundary conditions representative of a finite flat plate. In the present work, this solution is obtained using a boundary element method (BEM) accelerated by a fast multipole method (FMM) (Wolf and Lele, 2011)). The BEM uses Lighthill's stress tensor as an input to compute the scattered acoustic pressure by the finite plate. Once this scattered pressure is obtained, the BEM formulation becomes identical to Curle's equation.

2. EXPERIMENTAL SETUP

The jet-wing configuration, shown schematically in figure 1, is similar to that of Mead and Strange (1998), with a flat plate positioned in the vicinity of a round jet. The flat plate has length $L_x = 9D$ in the direction of the jet axis, a thickness of $L_y = 0.06D$ and a span $L_z = 15D$, where $D = 0.05$m is the jet diameter. The flat plate was placed with its trailing edge distance of $x_p = 5.5D$ to the exit plane of the jet. This value corresponds to the end of the potential core for the present jets (Cavalieri *et al.*, 2012b), and is an axial station where wavepackets in jets have significant amplitudes.

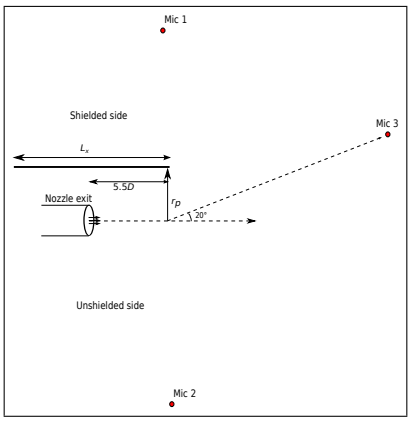

Figure 1. Schematic representation of the experimental setup

Due to the geometry of the problem at hand, we use a number of coordinate systems in the present work. A Cartesian system (x, y, z) is centered on the nozzle exit, where x is the jet axis, y is the transverse coordinate which is orthogonal to the plate, and z is parallel to the trailing edge of the plate. The velocity field of the jet is naturally defined in cylindrical coordinates (x, r, ϕ) where r is the radius and ϕ is the azimuthal angle. Finally, the acoustic field is expressed in spherical coordinates (R, Φ, θ), where R is the radius, Φ is the azimuth and θ is the polar angle; the latter is measured from the downstream axis of the jet. The spherical coordinate system has its origin at $x = 5.5D$ from the nozzle exit.

The microphone setup is also shown in figure 1. Two microphones are placed at $\theta = 90°$ and $R = 30D$ from the origin of the spherical coordinate system; one is placed at the shielded side of the plate and the other at the unshielded side. The microphones are set up in this way so that the phase opposition between the two sides of the plate can be easily identified. A third microphone is placed at $\theta = 20°$ on the shielded side of the jet. Measurements are performed over the acoustic Mach number range $0.4 < M < 0.6$ for a range of jet-wing distances $1 < r_p/D < 2$, where r_p is the distance between the plate and the jet axis. The Mach number range corresponds to previous work on free jets (Cavalieri *et al.*,

ISSN 2176-5480

2012b,a). Flow measurements are made using a Pitot probe and a hot wire. Details of the measurement system and data processing can be found elsewhere (Cavalieri *et al.*, 2012b).

3. ACOUSTIC RESULTS

3.1 Increase of sound radiation due to the flat plate

Figure 2 shows sound spectra measured by two diametrically opposed microphones at the sideline direction for different jet-wing distances and exit Mach numbers. A low-frequency amplification can be observed, similar to that observed by Mead and Strange (1998) and Lawrence *et al.* (2011), for both the shielded and unshielded microphones and for all Mach numbers. The shielding effect of the flat plate is observed only in the higher frequencies (at He>0.2). The amplified part of the spectra scales better when plotted as a function of Helmholtz number, showing that the related mechanism is associated with the ratio between the characteristic length of the problem and the acoustic wavelength, rather than with some change in the turbulence of the jet.

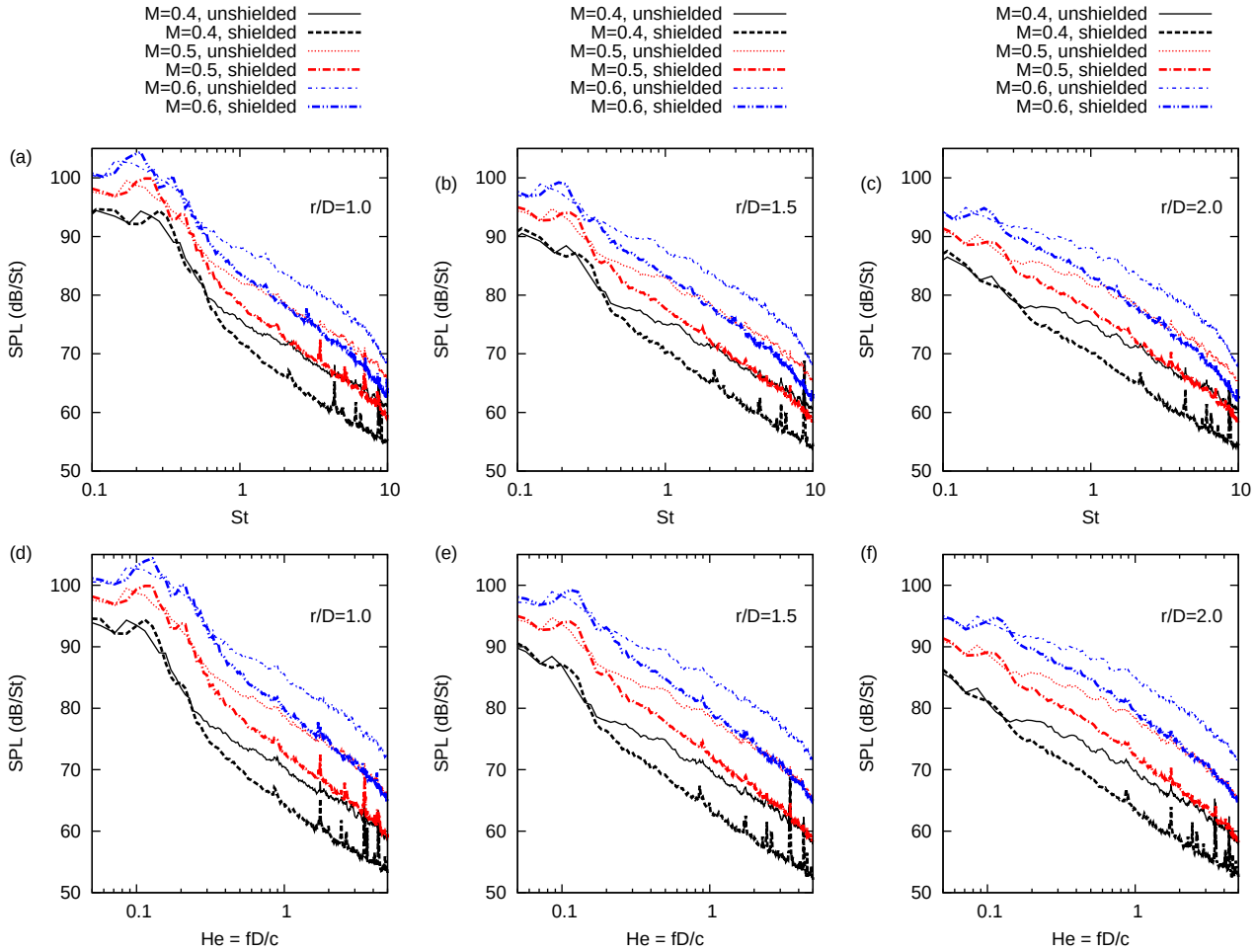

Figure 2. Sound spectra measured by the shielded and unshielded microphones for $r_p/D = 1$ (*a* and *d*), $r_p/D = 1.5$ (*b* and *e*) and $r/D = 2$ (*c* and *f*). Spectra are shown as a function of Strouhal number (top row) and Helmholtz number (bottom row).

Figure 3 compares the unshielded spectra, for r_p/D=1, 1.5 and 2, with that of the free jet. The fact that the high frequency part of the former does not perfectly match that of the free jet with an additional 3dB (to account for uncorrelated reflection of the sound field) is believed to be due to the fact that the plate dimensions are finite (3dB would result from reflection by an infinite plane). Also of note in this figure is the dependence of the amplified part of the spectrum on the jet-wing distance: variation of the SPL with r_p/D is exponential, suggesting that the fluctuations driving the amplified part of the sound field are those of the hydrodynamic jet nearfield, whose radial decay is also exponential (Crighton and Huerre, 1990; Suzuki and Colonius, 2006).

ISSN 2176-5480

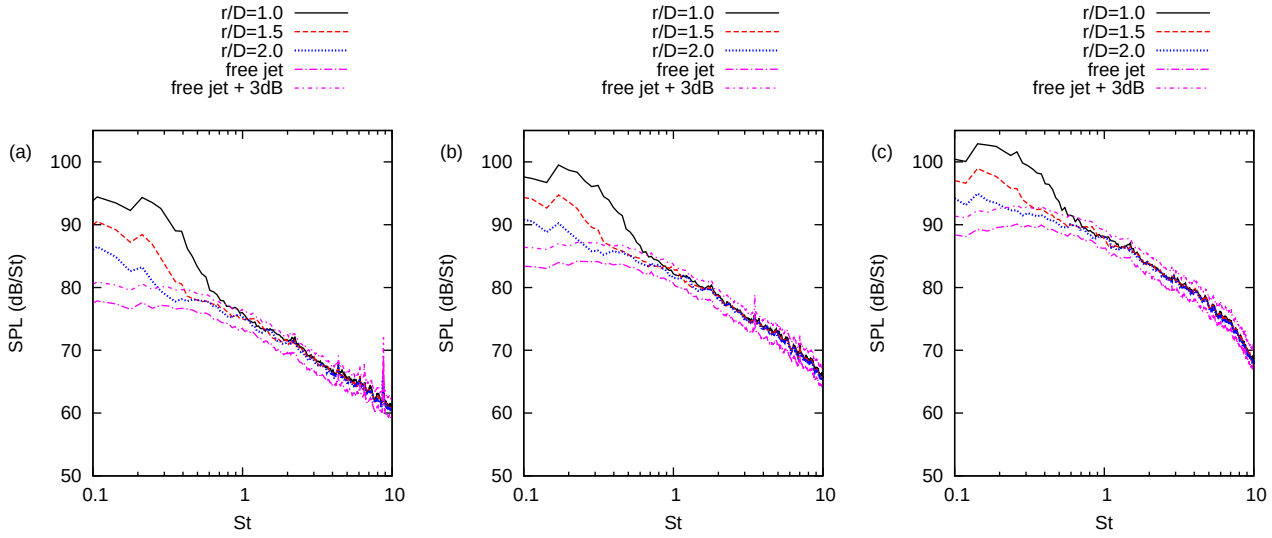

Figure 3. Effect of distance between the plate and the jet centerline on sound radiation for unshielded microphones at $\theta = 90°$ the $M = 0.4$ (a), $M = 0.5$ (b) and $M = 0.6$ (c) jets

3.2 Evaluation of scattering by the plate trailing edge

The low-frequency amplification was postulated by Mead & Strange to be due to the scattering of the jet by the trailing edge. While the above observations support this hypothesis, further verification can be obtained by considering the coherence between pressure signals of the two diametrically-opposed microphones. As the scattering mechanism leads to phase opposition between shielded and unshielded sides, as we will see in section 4.3, the two microphones should be highly correlated at the scattered frequencies, and, furthermore, a particular phase relationship should exist. The coherence between the microphones is shown in figure 4 for different jet-wing distances and Mach numbers. The coherence is consistently high (varying from 0.6 to 0.9) in the frequency range corresponding to the sideline amplification seen in figure 3.

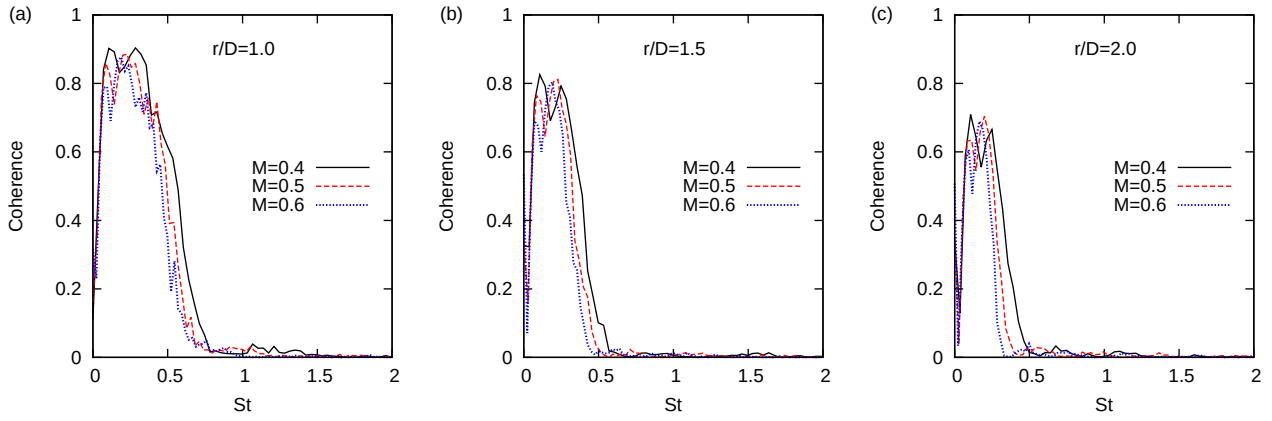

Figure 4. Coherence between signals from two diametrically-opposed microphones at $\theta = \pm 90°$ for $r/D = 1$ (a), $r/D = 1.5$ (b) & $r/D = 2$ (c).

As the microphones are centered on the jet axis, for a distance r_p between the plate and the axis the phase difference between the microphones, supposing that there is phase opposition between the shielded and unshielded sides, is given as

$$\Delta\psi = -\pi + 4\pi \mathrm{St} M \frac{r_p}{D}. \tag{1}$$

This phase characteristic is compared with the experimentally-determined phase in figure 5. The straight lines show the model in eq. (1). Close agreement is observed between the modelled and measured phase over the frequency range corresponding to the sideline amplification.

3.3 Investigation of wavepacket scattering

The results in sections 3.1 and 3.2 suggest that the increase of the acoustic intensity at the sideline direction is due to

ISSN 2176-5480

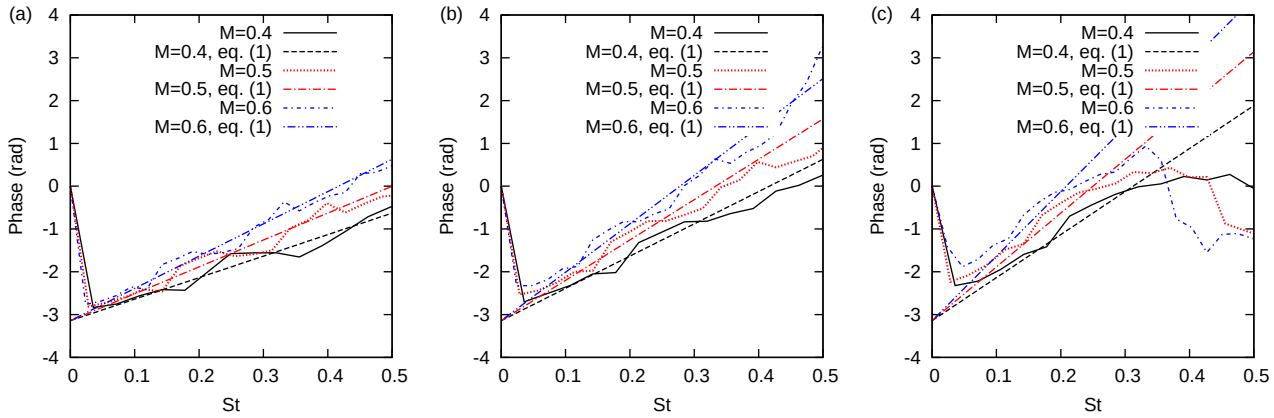

Figure 5. Phase difference between the two microphones for (*a*) $r_p/D = 1$, (*b*) $r_p/D = 1.5$ and (*c*) $r_p/D = 2$.

scattering at the plate trailing edge. The exponential dependence of the acoustic intensity with r_p, shown in section 3.1, indicates that such scattering may be related to wavepackets in the jet. For free subsonic jets, there is evidence that sound emission at low polar angles is related to wavepackets (Reba *et al.*, 2010; Cavalieri *et al.*, 2012b,a). However, at present it is not clear if the sound radiated at higher angles is also due to wavepackets in the jet. Correlations between far-field sound at $\theta = 30°$ and $\theta = 90°$ are nearly zero (Maestrello, 1977), which raises a doubt concerning the acoustic efficiency of wavepackets for radiation in the sideline direction. On the other hand, the presence of a scattering surface can enhance wavepacket radiation at high polar angles. We investigate this in the present section by comparing the correlations between far-field sound at $\theta = 90°$, which for installed jets is dominated by the scattered sound, and $\theta = 20°$, an angle where most of the sound from the isolated jet is axisymmetric and can be modelled as wavepacket radiation (Cavalieri *et al.*, 2012b,a).

Figure 6 presents correlation coefficients and coherences calculated from the acoustic pressure measured at $\theta = 20°$ and $90°$. In figure 6(a), we note that for the free jet the correlation between shallow-angle and sideline radiation is within the noise level, in agreement with the results of Maestrello (1977). However, for jets in the vicinity of a flat plate, significant correlations are found, which tend to be higher for smaller jet-plate distances.

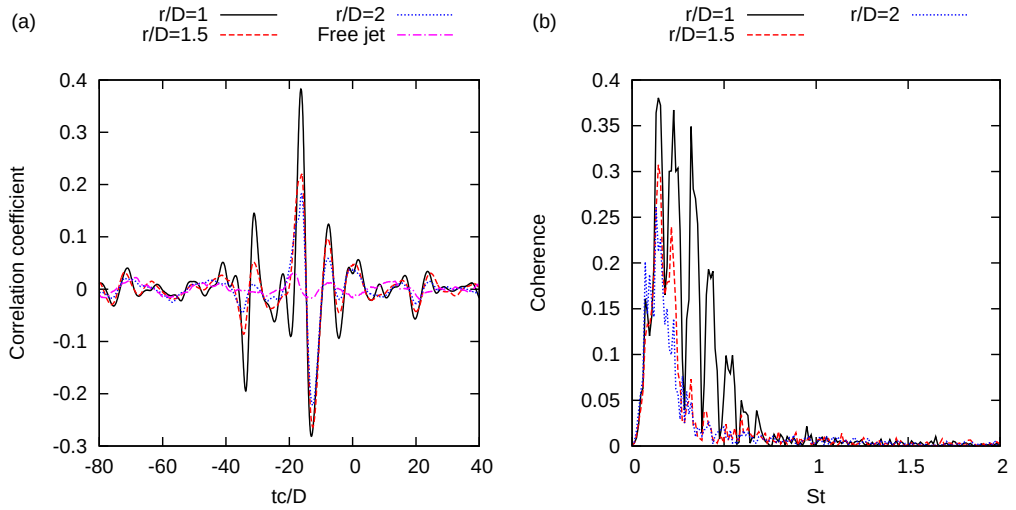

Figure 6. Investigation of wavepacket scattering in the acoustic field of the $M = 0.6$ jet: (a) Correlation coefficients and (b) coherence between far-field sound at $\theta = 20°$ and $90°$.

For the installed jets, the coherence between $\theta = 20°$ and $90°$ is shown in figure 6(b). As expected from the correlation results, coherence tends to be highest for low jet-plate distances. The Strouhal numbers with significant coherence correspond to the part of the spectra significantly enhanced by scattering, as shown in section 3.1. A feature of figure 6(*a*) is the presence of multiple peaks of the correlation. As will be seen in section 4.3, all four edges of finite plate scatter acoustic waves. We attribute the multiple peaks in the correlation to the scattering by the different edges of the plate, each extremity being related to a correlation peak. The above analysis of the acoustic results suggests that the increase of sound radiation in the sideline direction is due to the scattering of wavepackets by the plate edge. In the following section we evaluate this possibility using two modelling approaches.

ISSN 2176-5480

4. A MODEL FOR SOUND RADIATION BY A JET CLOSE TO A FLAT PLATE

4.1 Source model

With a view to modelling the noise source mechanisms corresponding to the scattering of the hydrodynamic nearfield by the plate, we use a source shape educed from far-field measurements of the present jets without the presence of the flat plate (Cavalieri *et al.*, 2012a). We use a simplified wavepacket source given by

$$T_{xx}(x,r,m,\omega) = 2\rho_0 \bar{u}_x(r)\hat{u}_x(r,m,\omega)^{-k_H x - \frac{x^2}{L^2}} \tag{2}$$

where $\bar{u}_x(r)$ was taken as the mean velocity profile at $x = D$, and the velocity fluctuations $\hat{u}_x(r,m,\omega)$ were modelled as linear instability waves of frequency ω and azimuthal mode m, using as a base flow the mean velocity profile at $x = D$. The axial wavenumber k_H was also determined using linear stability results.

The width of the Gaussian envelope is related to L, and the linear stability eigenfunction $\hat{u}_x$ has a free constant. These two parameters were educed from measurements of the far-field pressure resolved in azimuthal modes for the jet without the flat plate, and calculation of the radiated sound using Lighthill's analogy without surface effects led to close agreement between model and experiment for low polar angles (Cavalieri *et al.*, 2012a). We study these sources, educed using experiments without installation effects, to evaluate how the flat plate changes the radiated sound.

4.2 Acoustic predictions

The acoustic predictions are performed on one hand by means of a tailored Green's function $G(\mathbf{x},\mathbf{y},\omega)$ (Macdonald, 1915; Ffowcs Williams and Hall, 1970) that accounts for the presence of a semi-infinite, rigid flat plate, and, on the other, by solution of the Helmholtz equation with boundary conditions representative of a finite flat plate. The solution of the Helmholtz equation is obtained using a boundary element method (BEM) formulation accelerated by a fast multipole method (FMM) (Wolf and Lele, 2011).

The far-field pressure for the Ffowcs Williams & Hall formulation is obtained as

$$p(\mathbf{x},\omega) = \int_{\mathcal{V}} \frac{\partial^2 T_{ij}}{\partial y_i \partial y_j}(\mathbf{y},\omega) G(\mathbf{x},\mathbf{y},\omega) \mathrm{d}\mathbf{y}, \tag{3}$$

where $\mathbf{x}$ and $\mathbf{y}$ are the positions of observer and source, respectively, T_{ij} represents the components of Lighthill's stress tensor and ω is the angular frequency. The tailored Green's function G for a rigid, semi-infinite flat plate is given by Ffowcs Williams and Hall (1970). The far-field solution for the free jet is obtained using the free-field Green's function $G_0(\mathbf{x},\mathbf{y},\omega)$ instead of G in equation (3).

Most of the analysis of Ffowcs Williams and Hall (1970) supposed compact sources, i.e. isolated turbulent eddies. When such a source is near the edge of the plate, an increase of the radiated sound given by $(k\overline{r_0})^{-3}$ is found, where $\overline{r_0}$ is the distance from the center of the eddy to the plate edge. This algebraic increase can be seen, as discussed by Crighton *et al.* (1992), chapter 11, as a transformation of near-field into far-field energy. In the present work we wish to study scattering of non-compact sources, such as the wavepackets defined in section 4.1

The acoustic pressure for the Helmholtz equation implemented in the context of a BEM formulation is obtained as

$$c(\mathbf{x})p(\mathbf{x},\omega) = -\int_{\mathcal{S}} \frac{\partial G_0}{\partial n_y}(\mathbf{x},\mathbf{y},\omega) p(\mathbf{y},\omega) \mathrm{d}\mathbf{y} + \int_{\mathcal{V}} \frac{\partial^2 T_{ij}}{\partial y_i \partial y_j}(\mathbf{y},\omega) G_0(\mathbf{x},\mathbf{y},\omega) \mathrm{d}\mathbf{y}, \tag{4}$$

where $c(\mathbf{x})$ is equal to $1/2$ when $\mathbf{x}$ is on a boundary element surface $\mathcal{S}$ and $c(\mathbf{x})$ is equal to 1 when $\mathbf{x}$ is in the acoustic field. The term $\partial(.)/\partial n_y$ represents an inward normal derivative computed at a boundary element $\mathbf{y}$. In the present work, rigid surface boundary conditions are specified on the surface of the flat plate, $\partial p/\partial n_y = 0$. One should note that the Sommerfeld radiation condition, which allows only solutions with outgoing waves at infinity to be admitted, $\lim_{r\to\infty} r\left(\partial p/\partial n - ikp\right) = 0$, is naturally satisfied for the BEM formulation along a surface in the farfield, $\mathcal{S}_{inf}$.

4.3 General properties of the radiated sound field

An example of the sound field generated by a wave-packet source defined by eq. (2) in the presence of a semi-infinite flat plate is shown in figure 7. We note the expected pressure jump between the two sides of the plate, which in the figure corresponds to $x < 0$ and $y = D$. Scattering of the wavepacket by the plate trailing edge leads to sound radiation in all directions, with a phase opposition between the two sides of the plate in the sideline direction, in agreement with the experimental results shown in section 3.2

When a wavepacket is scattered by a finite flat plate, the four edges of the plate and the four corners lead to scattering effects. An example of this, for a single corner, is the problem of diffraction of a plane wave by quarter-plane (see Assier and Peake (2012) and references therein), which leads to a scattered field with a combination of conical waves scattered by the edges and a spherical wave scattered by the corner. Figure 8 illustrates the scattering of a wavepacket by a finite

ISSN 2176-5480

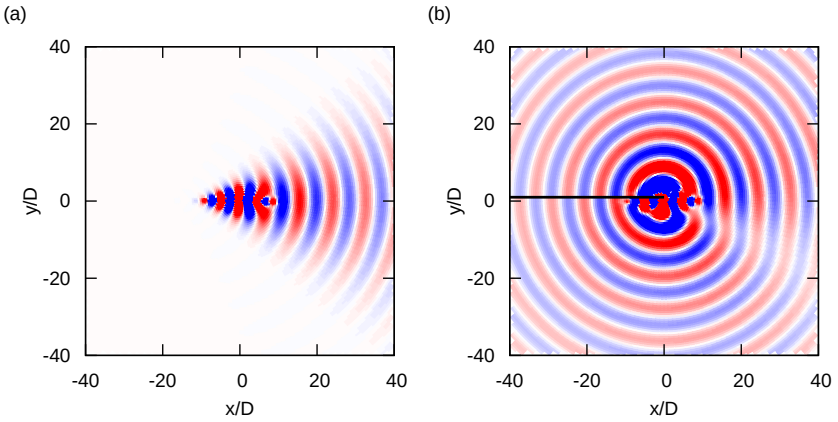

Figure 7. Pressure field for a wave-packet source with $k_H L = 6$, $M = 0.6$, $U_c/U = 0.97$ and $\mathrm{St} = 0.2$ (a) in free field and (b) with a semi-infinite flat plate at $x < 0$, $y = 1.0D$.

plate; the solution was obtained numerically with the methods described in section 4.2 . We see in figure 8(b), showing the total acoustic field, that the acoustic pressure has a more complex directivity pattern; it is nonetheless easy to identify scattering by the multiple edges of the plate, which lead to zero amplitudes in the plate plane and to an interference pattern between waves scattered on each edge. The phase opposition between shielded and unshielded sides is still present.

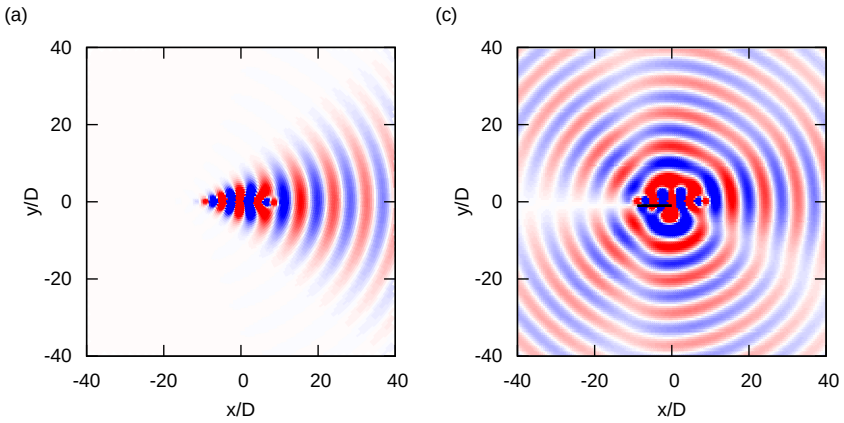

Figure 8. Pressure field for a wave-packet source with $k_H L = 6$, $M = 0.6$, $U_c/U = 0.97$ and $\mathrm{St} = 0.2$ (a) in free field and (b) total (incident plus scattered) acoustic field for a wavepacket with a finite flat plate at $y = 1.0D$

For small distances between the plate and the wavepacket, as in figures 7 and 8, the plate is in the near field of the source. To understand the scattering mechanism for these small distances, and the resulting dependence of the scattered sound, it is useful to study the near field of wavepackets without the plate. As discussed by Crighton and Huerre (1990), for wave-packet sources without surface effects the pressure amplitudes decay exponentially with increasing radius in the near field. As the distance from the source is increased, the decay switchs to algebraic, given by r^{-1} in the far acoustic field. On the other hand, for compact sources, the exponential decay in the near-field is not observed. This is exemplified in figure 9, where we have used different values of $k_H L$ for the source defined by eq. (2). Low values of $k_H L$ lead to compact sources without spatial oscillations, whereas high $k_H L$ is related to non-compact wavepackets. We note in figure 9 (a) the expected exponential decay of pressure amplitudes with increasing distance for the wave-packet sources. For high distances the amplitudes present algebraic decay. Higher values of $k_H L$ lead to exponential decays extending several jet diameters in the near field. On the other hand, a compact source, illustrated by the $k_H L = 0.5$ case, presents algebraic decay on both its near and far fields; the near pressure field decays with r^{-3}, and for higher distances the acoustic decay of r^{-1} is observed, as shown in figure 9(b).

When scattering by the flat plate is accounted for, the dependence of the far-field sound on the distance between the plate and the jet reflects the difference in the near-field decay between compact and non-compact sources. To study this, we have calculated the sound radiation by a semi-infinite flat plate, using eq. (3) with the wave-packet model of eq. (2).

ISSN 2176-5480

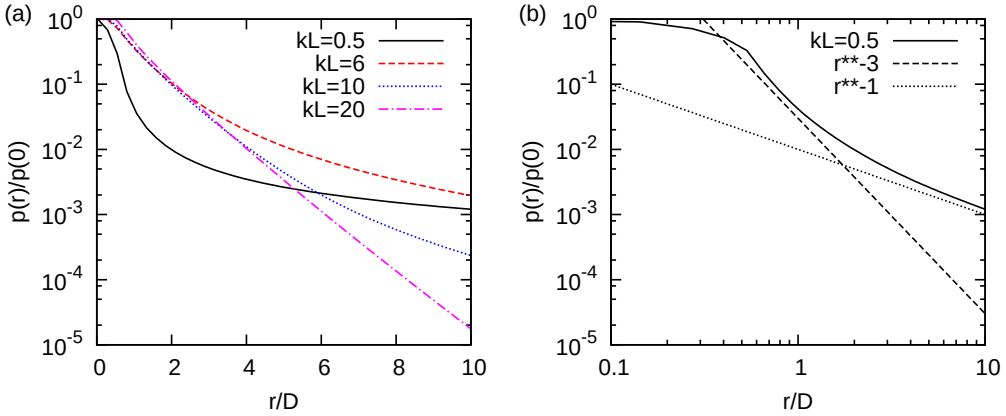

Figure 9. Pressure amplitudes calculated with wave-packet sources with $M = 0.6$, $U_c/U = 0.97$ and $\mathrm{St} = 0.2$ without surface effects, following a line at $\theta = 60°$ in (*a*) semilog and (*b*) log-log axes.

Figure 10 shows the dependence of the radiated sound at $\theta = 90°$ by wave-packet sources as a function of the position of the plate. We note that the non-compact wavepackets, with $k_H L = 6$ and higher, lead to an *exponential* dependence of the radiated sound with the jet-plate distance. For a compact source, exemplified with $k_H L = 0.5$, the dependence is algebraic, as predicted by Ffowcs Williams and Hall (1970). For small distances to the jet axis, the presence of a semi-infinite flat plate in the near-field of a wavepacket increases thus the radiated sound by a conversion of the near-field energy into radiated sound. The exponential decay of the near-field amplitudes is reflected in the exponential dependence of the scattered sound on the jet-plate distance.

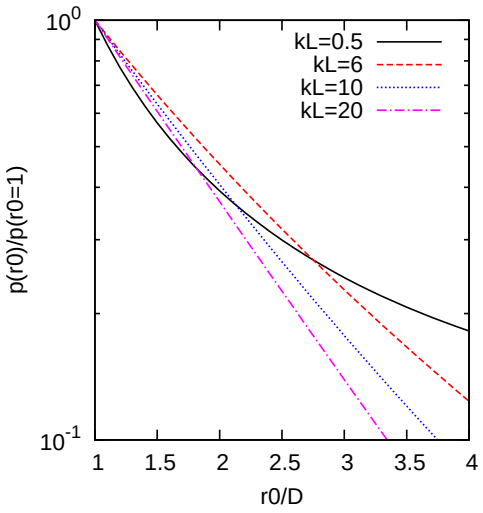

Figure 10. Pressure amplitudes at $R = 35D$ and $\theta = 90°$ calculated with wave-packet sources with $M = 0.6$, $U_c/U = 0.97$ and $\mathrm{St} = 0.2$ scattered by a semi-infinite flat plate distant r_p from the jet axis.

4.4 Comparison of model results

To compare our models with the experimental results, we use both the tailored Green's function approach, which amounts to supposing the flat plate to be semi-infinite with zero thickness, and the solutions of the Helmholtz equation for a finite plate. These numerical solutions for the finite flat plates are conducted using the FMM-BEM for plates with different chord and span dimensions in order to assess the effects of scattering by the trailing, leading and lateral edges. Dimensions are chosen to mimic the experiment, $L_x/D = 9$, $L_y/D = 0.06$, $L_z/D = 15$, and for flat plates with a larger chord and the same span, $L_x/D = 18$, $L_y/D = 0.06$, $L_z/D = 15$, larger span and the same chord, $L_x/D = 9$, $L_y/D = 0.06$, $L_z/D = 30$, and larger chord and span, $L_x/D = 18$, $L_y/D = 0.06$, $L_z/D = 30$. With these test cases, one should be able to discern the scattering effects by the multiple plate edges. For all flat plates investigated, a mesh convergence study was performed and results are shown for converged solutions.

The source model for both computations is the axisymmetric wavepacket of eq. (2) with parameters fitted using the same jets (Cavalieri *et al.*, 2012a), but without the flat plate, as discussed in section 4.1. In Fig. 11 we compare results for the sound radiation with those obtained from the experimental measurements. All directivity results in this section are

ISSN 2176-5480

calculated at $R = 35D$.

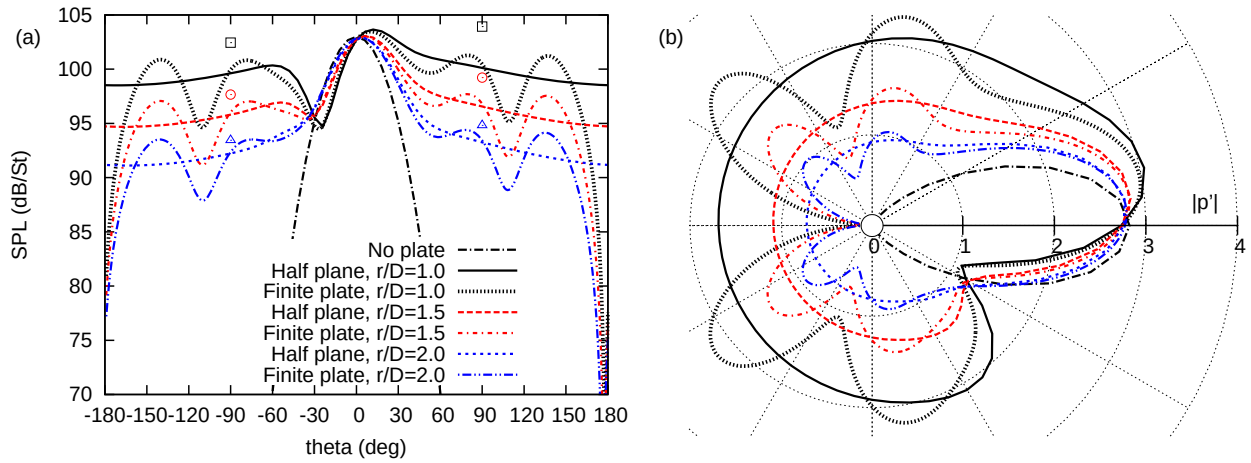

Figure 11. (*a*) Comparison of directivity for $\mathrm{St} = 0.2$ between models (half plane: Ffowcs Williams & Hall; finite plate: solution of Helmholtz equation) and experiment for the $M = 0.6$ jet. Squares, circles and triangles are experimental results for $r_p/D = 1.0$, 1.5 and 2.0, respectively. (*b*) Polar comparison of acoustic pressure obtained by Ffowcs Williams & Hall formulation and for the Helmholtz equation. Dimensions of the finite flat plate are identical to those tested in the experiments

Both models show an exponential dependence of the radiated sound on the jet-plate distance in agreement with experiments. However, numerical results are in all cases slightly lower than experimental measurements, a difference which may be due to the fact that the source model comprises only the axisymmetric mode. We expect that helical wavepackets, which are also present in the jet (Suzuki and Colonius, 2006; Gudmundsson and Colonius, 2011), will also be scattered by the plate and, therefore, will have a contribution to the sound at $\theta = 90°$. The present results encourage further measurements to evaluate source properties and to provide the directivity of scattered sound. Figure 11 also shows a comparison of results in terms of directivity plots for the semi-infinite and finite flat plates. Dimensions of the finite flat plate are identical to those used in the experiments. In Fig. 11 (a) and (b), one can see a comparison of SPL and acoustic pressure, respectively, obtained by the Ffowcs Williams & Hall formulation and for the Helmholtz equation. Results show good agreement for the scattered sound. Sound pressure levels for different r_p/D also present good comparison. However, one can observe the appearance of additional lobes in the directivity plots obtained for the finite plate due to additional diffraction effects (Assier and Peake, 2012) that occur on the leading and lateral edges of the plate.

A comparison of directivities in terms of SPL and acoustic pressure is presented in Fig. 12 for flat plates with different dimensions at $r_p/D = 1$. One can observe that increasing the span of the flat plate while keeping the same chord used in the experiment reduces the amplitudes of the lobes. However, the positions of these lobes are unaltered. When the chord length is increased, both the positions and amplitudes of the lobes are considerably changed and the main lobes move to lower angles towards the leading edge of the plate. One can also see that finite plate results slowly approach that of the semi-infinite flat plate when both chord and span of the plate are increased.

In Fig. 13(*a*), we assess the effects of each noise source mechanism present on the solution of the Helmholtz equation. The directivities of the incident acoustic field and of the scattered field are shown for a flat plate with the same dimensions as in the experiment, and for one with twice the dimensions of the chord and span. We can see the directivity changes due to trailing edge scattering for different chord lengths, and, therefore, different Helmholtz numbers, kL_x. It is expected that, for higher Helmholtz numbers, trailing edge scattering directivities start forming multiple lobes. One should also expect that the main lobes with higher amplitudes move to lower observer angles towards the leading edge (Wolf *et al.*, 2012). Figure 13(*b*) shows results of airfoil trailing edge scattering obtained by the Ffowcs Williams & Hawkings equation (Ffowcs Williams and Hawkings, 1969) for Helmholtz numbers similar to those considered in the present finite flat plate calculations. The overall directivity shapes are similar between the two problems, with multiple lobes for higher Helmholtz numbers. One should mention, however, that for the airfoil trailing edge scattering results, diffraction effects along lateral edges are not present.

Figure 14 presents azimuthal directivities measured at the flat plate trailing edge. Calculations are performed for the flat plates discussed in Fig. 13(*a*) and for the semi-infinite half plate. From this figure it is possible to observe the dipolar structure of sound radiation for the analysed plates. This dipolar pattern is slightly modified with the plate dimensions, but in all cases is close to the $\sin(\phi)$ directivity for the pressure amplitude. Ffowcs Williams & Hall's result, for compact sources, is also an azimuthal directivity of $\sin(\phi)$ for the pressure. The wavepackets used in our models can be approximated as radially compact. With this in mind, the present results suggest that for radially compact sources the azimuthal directivity on the sideline direction can be approximated by $\sin(\phi)$.

ISSN 2176-5480

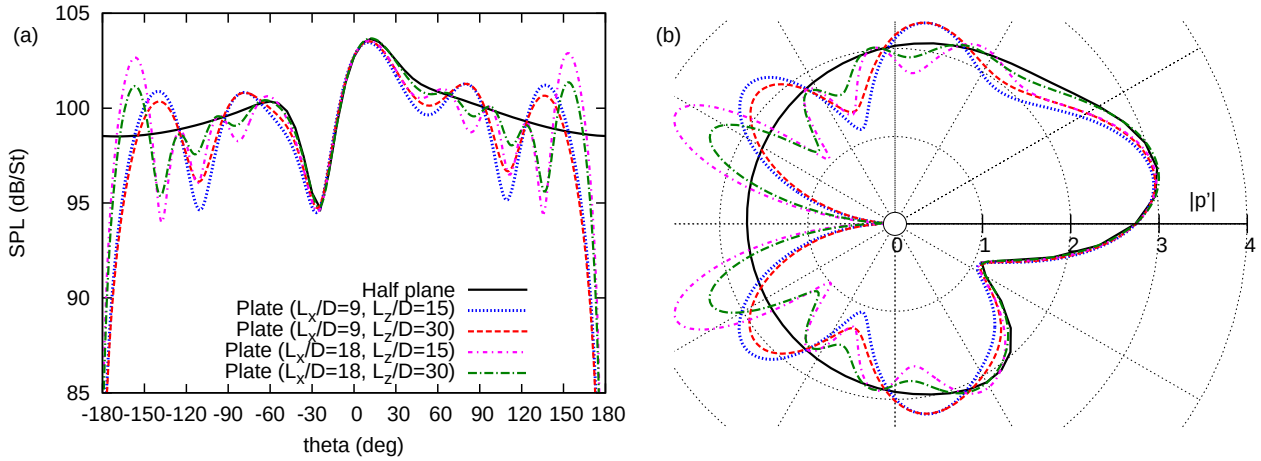

Figure 12. (a) Comparison of SPLs for flat plates with different dimensions at $r_p/D = 1$; (b) Polar comparison of acoustic pressure for flat plates with different dimensions

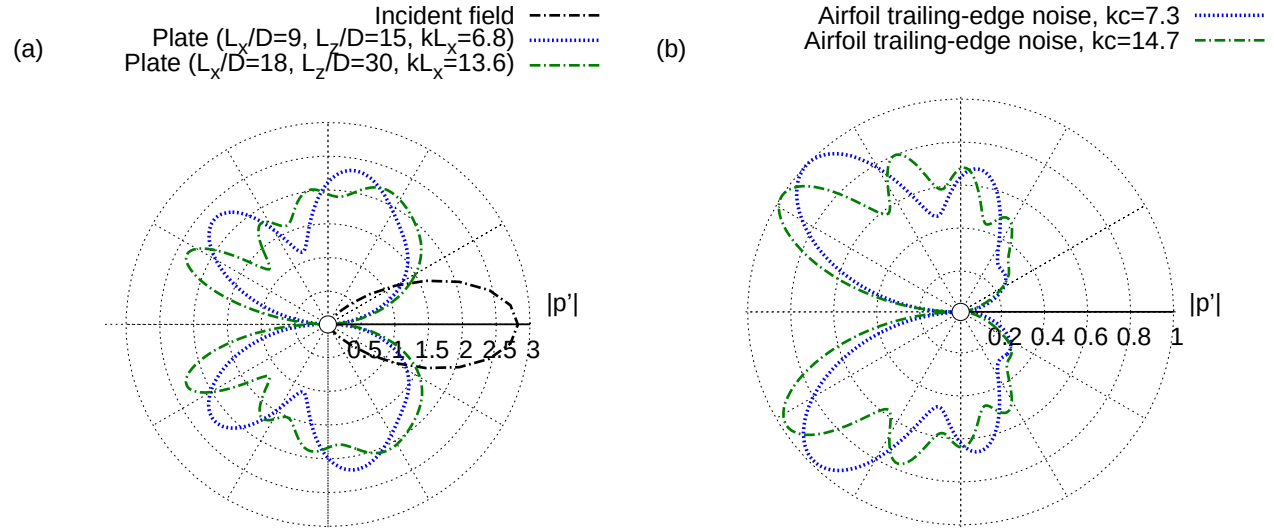

Figure 13. (a) Scattered field directivities for flat plates with different dimensions at $r_p/D = 1$; (b) Directivities obtained by Ffowcs Williams & Hawkings equation for airfoil trailing edge scattering

5. CONCLUSION

Experiments have been performed to explore the mechanisms involved in sound generation when a turbulent jet is situated in close proximity to a flat plate. The experimental setup constitutes a simplified representation of a jet-wing interaction, which is of concern to aircraft manufacturers. The results support the hypotheses that: (1) large sideline amplification in the sound field is due to scattering of the jet nearfield by the plate trailing edge; and, (2) that the jet nearfield comprises non-compact, hydrodynamic wave-packets.

The problem is modelled in two ways and results are compared with the experimental data. The source is modelled in both cases as an axisymmetric hydrodynamic wave whose radial structure is obtained from a linear stability analysis of the turbulent mean flow. The scattering problem is then solved for semi-infinite and finite plates. Scattering by the semi-infinite plate is computed using the tailored Green's function proposed by Macdonald (1915) and Ffowcs Williams and Hall (1970), whereas the more complex scattering problem associated with the finite plate is addressed via solution of the Helmholtz equation with boundary conditions that correspond to the real plate dimensions. This solution is obtained by means of a boundary element method accelerated by a fast multipole method.

Both approaches capture the two main characteristics of the sound field radiated by the jet-wing interaction: large low-frequency amplification, with dipolar directivity, and an exponential dependence of the radiated sound pressure on the plate-jet distance—a behaviour which would not occur if the source field were compact). The more complex, multi-lobed, radiation pattern associated with interference between sound fields scattered by the four edges of the finite plate is captured using the boundary element method, and, as the plate dimensions are increased, the BEM solution is found to

ISSN 2176-5480

|p'|=sin(phi)$|p'| \propto \sin(\phi)$

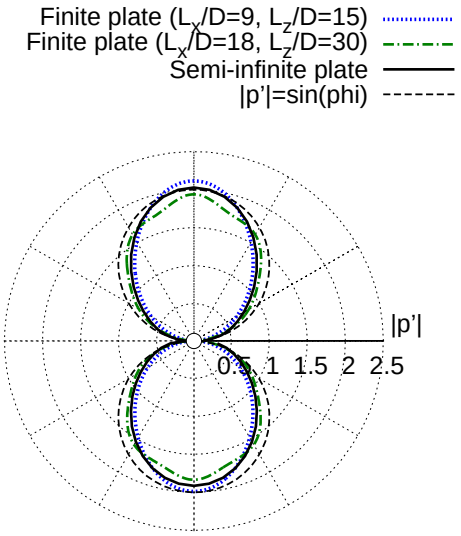

Figure 14. Azimuthal directivity for flat plates with different dimensions at $r_p/D = 1$

tend toward the semi-infinite plate solution.

6. ACKNOWLEDGEMENTS

This work is supported by CNPq, Brazil, and by the EU project JERONIMO (call reference number: FP7-AAT-2012-RTD-1; grant agreement number: 314692). The authors would like to acknowledge a useful discussion with Daniel Juvé regarding algebraic versus exponential decay of near-field fluctuations.

7. REFERENCES

Assier, R.C. and Peake, N., 2012. "On the diffraction of acoustic waves by a quarter-plane". *Wave Motion*, Vol. 49, pp. 64–82.

Cavalieri, A.V.G., Jordan, P., Colonius, T. and Gervais, Y., 2012a. "Axisymmetric superdirectivity in subsonic jets". *Journal of Fluid Mechanics*, Vol. 704, p. 388.

Cavalieri, A.V.G., Rodríguez, D., Jordan, P., Colonius, T. and Gervais, Y., 2012b. "Wavepackets in the velocity field of turbulent jets". In *18th AIAA/CEAS Aeroacoustics Conference and Exhibit*. Colorado Springs, CO, USA.

Crighton, D.G., Dowling, A.P., Ffowcs Williams, J.E., Heckl, M. and Leppington, F.G., 1992. *Modern methods in analytical acoustics: lecture notes*. Springer.

Crighton, D.G. and Huerre, P., 1990. "Shear-layer pressure fluctuations and superdirective acoustic sources". *Journal of Fluid Mechanics*, Vol. 220, pp. 355–368.

Crow, S.C., 2072. "Acoustic gain of a turbulent jet". In *Phys. Soc. Meeting*. Boulder, CO, USA.

Curle, N., 1955. "The influence of solid boundaries upon aerodynamic sound". *Proceedings of the Royal Society A*, Vol. 231, pp. 505–51.

Ffowcs Williams, J.E. and Hall, L.H., 1970. "Aerodynamic sound generation by turbulent flow in the vicinity of a scattering half plane". *Journal of Fluid Mechanics*, Vol. 40, pp. 657–670.

Ffowcs Williams, J.E. and Hawkings, D.L., 1969. "Sound generation by turbulence and surface in arbitrary motion". *Philosophical Transaction of the Royal Society of London, Series A, Mathematical and Physical Sciences*, Vol. 264, pp. 321–342.

Ffowcs Williams, J.E. and Kempton, A.J., 1978. "The noise from the large-scale structure of a jet". *Journal of Fluid Mechanics*, Vol. 84, pp. 673–694.

Gudmundsson, K. and Colonius, T., 2011. "Instability wave models for the near-field fluctuations of turbulent jets". *Journal of Fluid Mechanics*, Vol. 689, pp. 97–128.

Jordan, P. and Colonius, T., 2013. "Wave packets and turbulent jet noise". *Annual Review of Fluid Mechanics*, Vol. 45, pp. 173–195.

Lawrence, J.L.T., Azarpeyvand, M. and Self, R.H., 2011. "Interaction between a flat plate and a circular subsonic jet". In *17th AIAA/CEAS Aeroacoustics Conference and Exhibit*. Portland, OR, USA.

Lighthill, M.J., 1952. "On sound generated aerodynamically. i. general theory". *Proceedings of the Royal Society of*

ISSN 2176-5480

London. Series A, Mathematical and Physical Sciences, pp. 564–587.

Macdonald, H.M., 1915. "A class of diffraction problems". *Proceedings of the London Mathematical Society*, Vol. 2, p. 410.

Maestrello, L., 1977. "Statistical properties of the sound and source fields of an axisymmetric jet". In *American Institute of Aeronautics and Astronautics Conference*. USA.

Mankbadi, R. and Liu, J., 1984. "Sound generated aerodynamically revisited: large-scale structures in a turbulent jet as a source of sound". *Philosophical Transactions of the Royal Society of London. Series A, Mathematical and Physical Sciences*, Vol. 311, pp. 183–217.

Mead, C.J. and Strange, P.J.R., 1998. "Under-wing installation effects on jet noise at sideline". In *4th AIAA/CEAS Aeroacoustics Conference and Exhibit*. Toulouse, France.

Reba, R., Narayanan, S. and Colonius, T., 2010. "Wave-packet models for large-scale mixing noise". *International Journal of Aeroacoustics*, Vol. 9, pp. 533–558.

Suzuki, T. and Colonius, T., 2006. "Instability waves in a subsonic round jet detected using a near-field phased microphone array". *Journal of Fluid Mechanics*, Vol. 565, pp. 197–226.

Wolf, W.R., Azevedo, J.L.F. and Lele, S.K., 2012. "Convective effects and the role of quadrupole sources for aerofoil aeroacoustics". *Journal of Fluid Mechanics*, Vol. 708, pp. 502–538.

Wolf, W.R. and Lele, S.K., 2011. "Wideband fast multipole boundary element method: Application to acoustic scattering from aerodynamic bodies". *International Journal for Numerical Methods in Fluids*, Vol. 67, pp. 2108–2129.

8. RESPONSIBILITY NOTICE

The authors are the only responsible for the printed material included in this paper.